

# Adaption of the Mechanism of Emulsion Polymerization to New Experimental Results

Klaus Tauer,<sup>\*1</sup> Hugo F. Hernández,<sup>1</sup> Steffen Kozempel,<sup>1</sup> Olga Lazareva,<sup>1,2</sup>  
Pantea Nazaran<sup>1</sup>

**Summary:** New experimental investigations of the 'classical' batch ab-initio emulsion polymerization of styrene reveal the important role of monomer droplets for the whole process. Monomer droplets with a size between a few and some hundreds of nanometers, which are formed by spontaneous emulsification as soon as styrene and water are brought into contact, have a strong influence on the particle nucleation, the particle morphology, and the swelling of the particles. Experimental results confirm that micelles of low molecular weight surfactants are not a major locus of particle nucleation. Brownian dynamics simulations show that the capture of matter by the particles (monomer or radicals) strongly depends on the polymer volume fraction and the size of the captured species (primary free radicals, oligomers, single monomer molecules, or clusters).

**Keywords:** mechanism of emulsion polymerisation; particle nucleation; radical capture; swelling

## Introduction

Aqueous radical emulsion polymerization is the technically most important synthetic route to polymer dispersions and is used to produce worldwide about 7.5 million metric tons of dry polymer per year.<sup>[1]</sup> This contribution describes new experimental results aiming to provide a better experimental base for understanding emulsion polymerization. Particularly results will be presented regarding (1) particle nucleation in the absence and presence of both emulsifiers and seed particles, (2) the state of the monomer in water, and (3) the sorption of matter by latex particles.

## Experimental Part

The water was taken from a Seral purification system (PURELAB Plus) with a conductivity of  $0.06 \mu\text{S cm}^{-1}$  and degassed prior to use for the polymerization. Styrene (Aldrich) was distilled under reduced pressure to remove inhibitors. Potassium peroxydisulfate (KPS, Sigma Aldrich), sodium dodecyl sulfate (SDS, Roth), cetyl trimethyl ammonium bromide (CTAB, Ferak), 2, 2'-Azobis(2-methyl-butyronitrile) (V-59, Wako), and 2, 2'-Azobis(2-methyl-N-(2-hydroxyethyl)propionamide) (VA-086, Wako) were used as received. Azobisisobutyronitrile (AIBN, Fluka) was recrystallized from methanol before use. Poly(ethylene glycol)-azo-initiator (PEGA200) with an average molecular weight of 568 g/mol was synthesized as described elsewhere.<sup>[2,3]</sup>

The latexes were characterized regarding solids content with a HR73 Halogen Moisture Analyzer (Mettler Toledo) and average particle size (intensity weighted diameter) with a Nicomp particle sizer

<sup>1</sup> Max Planck Institute of Colloids and Interfaces, D-14476 Golm, Germany  
Fax: (+49) 331 567 9512;  
E-mail: klaus.tauer@mpikg.mpg.de

<sup>2</sup> Permanent affiliation: Lomonosov Moscow State Academy of Fine Chemical Technology, Prospect Vernadskogo 86, 119571 Moscow, Russia

(model 370, PSS Santa Barbara, USA). The polymer from the polymerizations in the presence of surfactant was isolated after freeze-drying the latex and washing the solid repeatedly with water. The zeta-potential ( $\xi$ ) and the z-average particle size ( $D_Z$ ) were determined according to standard procedures with Zetasizer 4 (Malvern). Molecular weight distributions were determined by gel permeation chromatography (GPC) in THF by standard procedure with a column set allowing a resolution down to molecular weights less than  $500 \text{ g mol}^{-1}$ . Number and weight average molecular weights ( $M_n$ ,  $M_w$ ) were calculated based on polystyrene standards (between  $500$  and  $2 \cdot 10^6 \text{ g mol}^{-1}$  from PSS, Mainz, Germany). Transmission electron microscopy (TEM) was performed with a Zeiss EM 912 Omega microscope operating at  $100 \text{ kV}$  and the samples were placed on the grids via suspension preparation. Optical light microscopy was carried out with a Keyence VH-X digital microscope (Keyence Corporation, Osaka, Japan) either with an objective VH-Z100 or VH-Z500 allowing magnifications up to  $1000$  and  $5000$ -fold, respectively. UV – fluorescence microscopy has been carried out with an OLYMPUS BX51 (Hamburg, Germany) with an excitation wavelength of  $330 - 385 \text{ nm}$ . Emission was detected in the wavelength range between  $400$  and  $420 \text{ nm}$ .

The kinetic investigations on particle nucleation were carried out in an all-Teflon reactor with a volume of about  $500 \text{ ml}$  connected to a UV spectrometer (Spekol 11, Carl Zeiss Jena) and equipped with a variety of probes to characterize the changes taking place in the aqueous phase as described in detail elsewhere.<sup>[4]</sup> During these experiments the stirring was adjusted so slowly that only the aqueous phase was homogenized without dispersing the monomer which is confined on top of the water phase in a glass funnel. A fibre optical quasi elastic light scattering probe (FOQELS) from Brookhaven Instruments Corp., USA wavelength  $785 \text{ nm}$  and scattering angle  $135,93^\circ$  was used in some experiments as described in.<sup>[5]</sup> These nucleation experi-

ments were carried out at  $70^\circ\text{C}$  according to the following procedure. In order to avoid bubble nucleation during the investigations the water was carefully degassed by vacuum treatment and boiled. It was filled in the reactor at a temperature above  $70^\circ\text{C}$ . In any case the temperature, the optical transmission (optical path length  $9,8 \text{ cm}$ ), and the conductivity were recorded. Surfactant-free emulsion polymerizations were carried out in an all-glass  $500 \text{ ml}$  reactor at  $70^\circ\text{C}$ . The experiments have been carried out either under quiescent conditions or with a stirrer speed of  $300$  revolutions per minute.

## Results and Discussions

### Detection of Particle Nucleation

Particle nucleation in *ab-initio* batch emulsion polymerizations starts at extremely low solids contents typically much below  $1\%$ . Thus, the experimental challenge to detect the onset and follow particle nucleation is quite significant. It turned out that conductivity is an extremely good tool to detect the onset of nucleation in surfactant-free polymerizations.<sup>[4,6–8]</sup> This established experimental base is illustrated by the data summarized in Figure 1. After allowing equilibration of the monomer in water the polymerization was started by injecting the

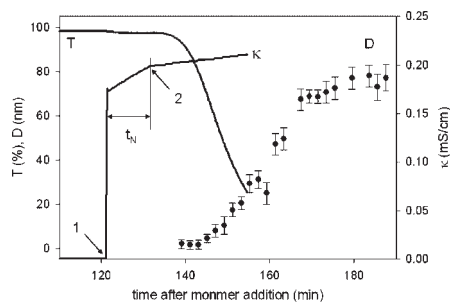


**Figure 1.**

Typical record of the initial period of surfactant-free emulsion polymerization of styrene initiated with KPS; on-line determination of transmission (T), conductivity ( $\kappa$ ), and average particles size (D, FOQELS); experimental conditions:  $70^\circ\text{C}$ ,  $400 \text{ g}$  of water,  $3.3 \text{ g}$  of styrene,  $0.054 \text{ g}$  of KPS.

initiator solution at point 1. The conductivity rises sharply and afterwards it increases, due to the decomposition of the peroxodisulfate, linearly with time during a definite period of time ( $t_N$ ).<sup>[6]</sup> Suddenly at point 2, within one second to the other, the slope of the conductivity - time curve changes to smaller value. This bend is the point where massive particle nucleation takes place and  $t_N$  denotes the nucleation time or the duration of the pre-nucleation period. The change of the slope takes place as mobile conducting species loose mobility due to incorporation in the electrical double layer of the particles. Independent proof that the bend marks nucleation comes from the fact that particles have only been detected with the FOQELS after the bend, almost at the same time when transmission starts to decrease. The smallest particles detected with the FOQELS have a diameter below 5 nm (between 2 and 3 nm) and compose of oligomers with an average molecular weight of about 600 g/mol. These particles contain between 4 and 15 oligomers and hence, they prove the aggregative nucleation model which was derived based on the classical nucleation theory.<sup>[7,9]</sup> Fitch and Watson reported already 1979 for photo-initiated methyl

methacrylate emulsion polymerization primary particles with a diameter of 3.8 nm that are composed of 3–4 oligomers with a chain length of 53.<sup>[10]</sup>

Surprisingly, if peroxodisulfate is substituted by non-ionic azo-initiators a very similar initial behavior is observed as illustrated by the data put together in Figure 2. These azo-initiators possess a quite different solubility in water but for all of them a bend in the conductivity - time curve occurs. Obviously, carbon radicals undergo in water side oxidation reactions leading to ionic species that increase the conductivity and stabilize the particles even in the absence of surfactants.<sup>[11]</sup> Note, V-59 has the lowest water-solubility and correspondingly, the change in the conductivity takes much longer (hours instead of minutes).

### Micellar Nucleation – Fact or Fancy

Harkins considered in 1947 three loci where the polymerization of the monomer can initiate polymer particles: the soap micelles, the aqueous phase, and the monomer droplets.<sup>[12]</sup> The smooth transition from a monomer swollen micelle to a polymerizing monomer - polymer particle is the core of the micellar particle formation mechanism as introduced by Smith and Ewart.<sup>[13]</sup>

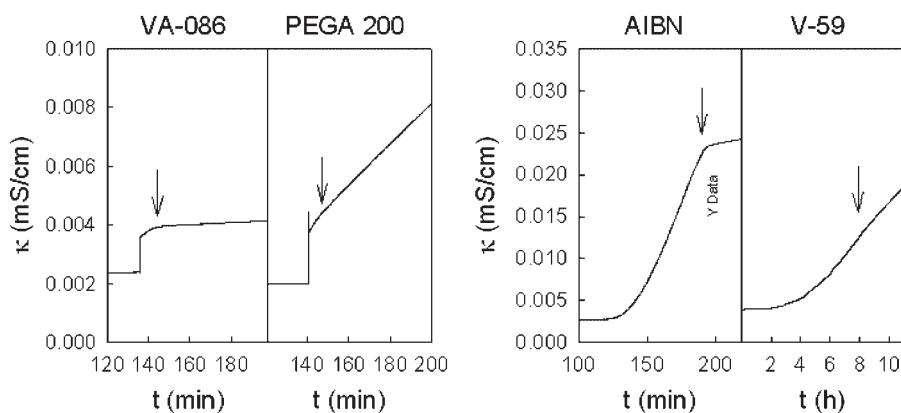


**Figure 2.**

Conductivity - time curves measured during the initial period of surfactant - free emulsion polymerization of styrene with different azo-initiators; the arrows indicate the bend in the curves; experimental conditions: 70 °C, 410 g of water and 3.3 g of styrene for VA-086 and PEGA200 or 400 g of water and 3.75 g of styrene for AIBN and V-59, respectively, the following amounts of initiator were added 120 minutes after placing the monomer on top of the water phase 0.072 g of VA-086, 0.112 g of PEGA 200, 0.075 g AIBN, 0.075 g V-59 (VA-086 and PEGA 200 were added as aqueous solution to water, AIBN and V-59 were added as solution in styrene to the monomer phase).

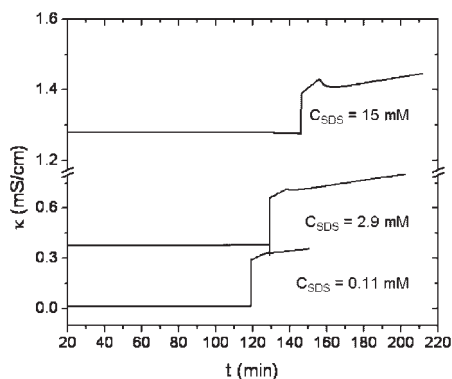


**Figure 3.**

Conductivity – time curves for emulsion polymerizations of styrene in the presence of various amounts of SDS; experimental conditions: 70 °C, 410 g of water, 0.064 g of KPS, 3.3 g of styrene; the CMC of SDS under these conditions is about 8 mM.

However until today, to the best of our knowledge, no experimental data are known in the open literature proving micellar nucleation unambiguously.

In the presence of absorbing particles, which can be either micelles or seed particles, the conductivity – time curves should possess a smooth pattern without sharp transitions, at least no bend towards smaller slopes should be observed, if no additional particles are formed (no secondary nucleation). Furthermore, a higher molecular weight in the low mass region of the molecular weight distribution can be expected as the swollen micelles are spots with higher monomer concentration in the aqueous phase. The conductivity data put together in Figure 3 show for SDS concentrations below and above the CMC a bend towards a lower slope. These experimental results prove that SDS micelles for styrene as monomer do not alter the nucleation behavior. Additionally, the molecular weight data

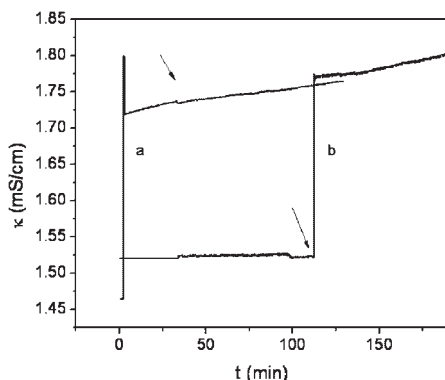


**Figure 4.**

Conductivity – time curves for emulsion polymerizations of styrene in the presence of seed particles with a volume fraction of 2%; the arrows indicate the start of the polymerization by monomer (a) and by KPS addition (b); experimental conditions: 70 °C, 410 g of water, 0.064 g of KPS, 3.3 g of styrene.

(cf. Table 1) give no hint that micelles are the locus where the initial polymerization reaction takes place. The molecular weight data in the low molecular weight region are independent of the SDS concentration. However, the average molecular weights in the high mass region of the molecular weight distribution strongly depend on the surfactant concentration. This is expected as the particles are the smaller the higher the SDS concentration and smaller particles imbibe less monomer.<sup>[14]</sup>

If instead of micelles seed particles are used as absorbing species it is possible to find a critical volume fraction of seed particles where the conductivity curves do not show secondary nucleation (cf. Figure 4). For the particular seed particles with an average size of 37 nm the critical volume fraction is between 0.2 and 2%. At the lower seed volume fraction a bend in the conductivity curve clearly proves secondary nucleation (data not shown here).

**Table 1.**

Average molecular weights of the high and low molecular mass region of polystyrene particles obtained in the presence of various amounts of SDS.

$C_{\text{SDS}}$ (mM)	$M_n/M_w$ (g/mol) (low molecular weight range)	$M_n/M_w$ (g/mol) (high molecular weight range)
0.11	360/480	$7.7 \cdot 10^4 / 1.2 \cdot 10^5$
2.9	280/600	$1.0 \cdot 10^4 / 2.4 \cdot 10^4$
13	360/700	none

However for a seed volume fraction of 2% the conductivity curve is a straight line without any sign of bending towards lower slope. This behavior was observed for both possibilities to start the polymerization that is either by the addition of styrene monomer or KPS. In the former case the monomer was added 30 minutes after KPS and in the latter case the system was equilibrated with monomer for two hours before starting the polymerization.

### Monomer Concentration and Particle Morphology

Besides the flux of primary radicals, adjusted either by the initiator concentration or

the temperature, the duration of the pre-nucleation period can also be controlled by the saturation of the aqueous phase with monomer. Varying the equilibration time of the aqueous phase with monomer from 0 to 480 minutes reduces  $t_N$  by about a factor of 7 and for monomer equilibration times longer than 5 h  $t_N$  is constant (5.7 minutes).

The identification of the monomer equilibration time as new experimental parameter influencing the particle nucleation kinetics raises immediately the question regarding the state of the monomer in water. It turned out that during the monomer equilibration period the transmission under the conditions of the standard

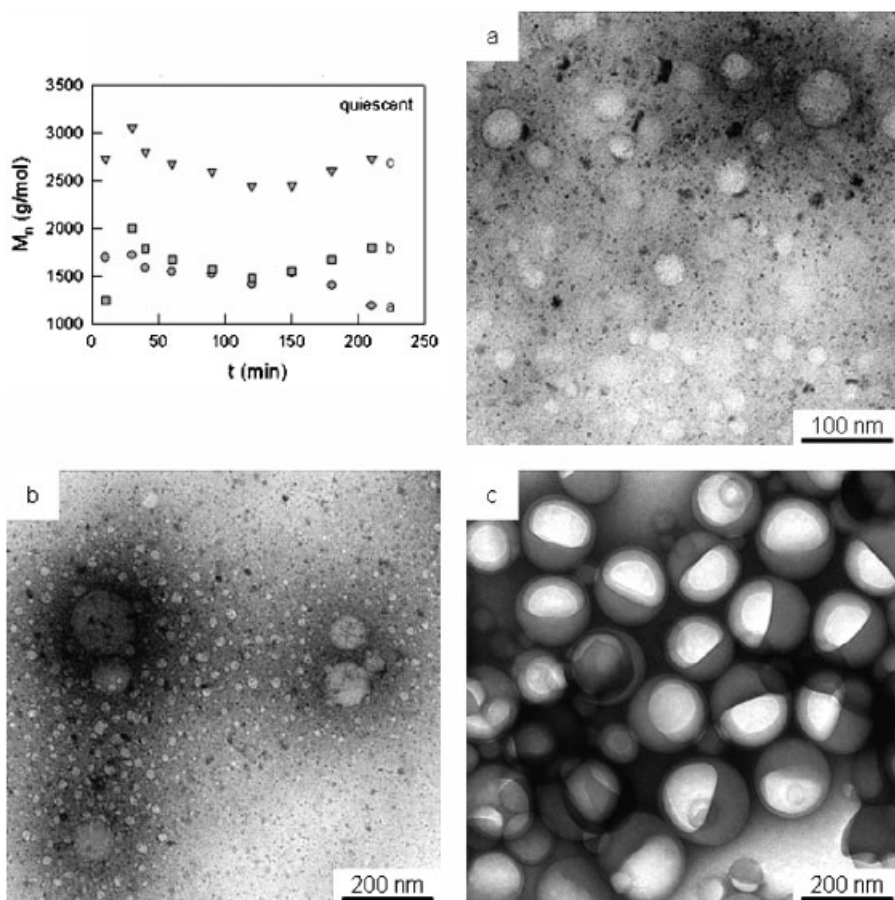


**Figure 5.**

Development of the number average molecular weights (upper left corner) and TEM images of the particle morphology (after polymerization time of 60 min) for surfactant-free emulsion polymerizations of styrene after monomer equilibration times of 0 (a), 30 (b), and 120 min (c); experimental conditions: all-glass reactor, non-stirred, 70 °C, 20 ml of styrene, 562.5 g of water, 1.25 g of KPS.

experiment decreases from 100 to about 91% continuously over about 3 h before reaching a constant value. With multi angle laser light scattering in glass cuvettes the development of a strong scattering signal in the aqueous phase was observed over a period of some hours after styrene was quiescently placed on top of the water.<sup>[15]</sup> These data indicate the formation of styrene droplets via spontaneous emulsification. Additional proofs for the existence of styrene droplets in a quiescent surfactant-free styrene in water system come from electron microscopy and light microscopy.<sup>[5,16]</sup> The consequence for the following polymerization is enormous as the huge interface facilitates monomer diffusion into water.

Despite their unimportance for the aqueous phase kinetics the monomer drops have a strong impact on the particle morphology. Figure 5 summarizes the influence of the duration of the monomer equilibration on the particle morphology and the average molecular weight. The average molecular weight is the higher the longer the duration of the monomer equilibration period and the TEM images reveal very special particle morphologies resembling rather vesicular or hollow particles than solid spheres.

Obviously, the monomer droplets formed after contacting styrene and water are templated or stabilized by small oligomeric particles. These oligomeric

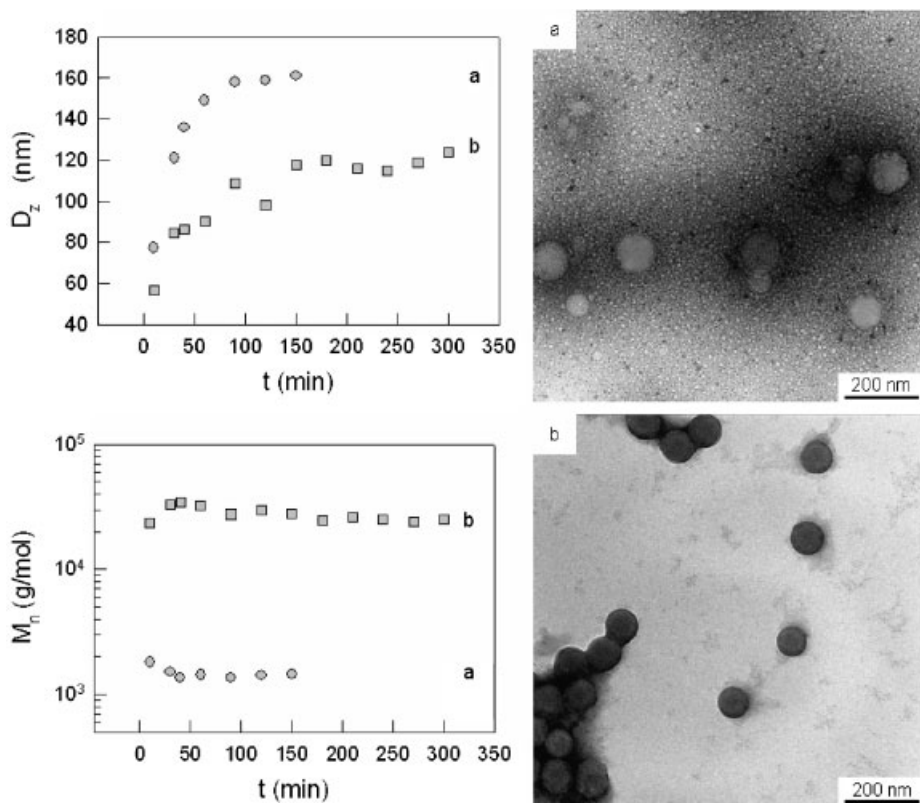


**Figure 6.**

Development of the average particle size ( $D_z$  from Zetasizer, upper left graph), the number average molecular weight ( $M_n$ , lower left graph), and TEM images of the particle morphology (after polymerization time of 30 min) for non-stirred surfactant-free emulsion polymerizations of styrene with 120 min monomer equilibration time; experimental conditions: all-glass reactor, 70 °C, 20 ml of styrene, 562.5 g of water, 1.25 g of KPS (a, grey circles) and 0.094 g of KPS (b, grey squares).

particles have a size below 5 nm and are visible as small dark spots on the TEM images. They consist of a few oligomers with higher electron density due to the greater sulfur and oxygen content and are insoluble in both the water and the monomer. This scenario can explain the experimental observations from the spontaneous emulsification to the formation of vesicular or hollow particles. If however, the polymerization conditions lead to oligomers with higher molecular weights, which are soluble in the droplets, solid particles are formed (cf. Figure 6).

### Absorption of Matter by Latex Particles

Due to their large surface area colloidal particles can effectively absorb or imbibe all kinds of materials of either hydrophobic or hydrophilic nature.<sup>[17]</sup> Radicals and monomers are for emulsion polymerizations of particular importance. Despite the actual situation that the uptake-mechanism of monomers and radicals is considered differently there are general principles involved which have to be considered.

It has been found that the Morton – Kaizerman – Altier (MKA) equation<sup>[18]</sup> is not suited to describe quantitatively the swelling of latex particles by organic solvents for the polymer.<sup>[19]</sup> In order to achieve a better agreement with experimental data a swelling pressure taking into account the work necessary for the disintegration of

entangled polymer molecules, the concentration dependence of the Flory – Huggins interaction parameter, and the dependence of the interfacial tension on the particle size have to be considered.<sup>[14]</sup> The investigation of swelling of large monodisperse latex particles by means of light microscopy revealed some new experimental facts which on the one hand have to be considered for improved theoretical description and on the other hand offer novel possibilities for the modification of latex particles.

Figure 7 reveals that the particles which are in closer contact to the oil phase swell at given time larger than those in farther distance from the interface.

For these particular polystyrene particles sitting in the first row it takes about 3–4 hours to reach the swelling equilibrium at room temperature. The data presented in Figure 7 and 8 are to the best of our knowledge the first determination of the swelling kinetics by evaluating the size increase of individual particles. The equilibrium volume fraction of ethyl benzene is about 0.9 corresponding to a swollen particle size of about 12  $\mu\text{m}$  which is in quite good agreement with the prediction of the MKA - equation if the interfacial tension is about 50 mN/m. However, this interfacial tension is surely much too high as it is only 32 mN/m between neat polystyrene and water.<sup>[20]</sup> This result points to the fact that the MKA-equation overestimates swelling

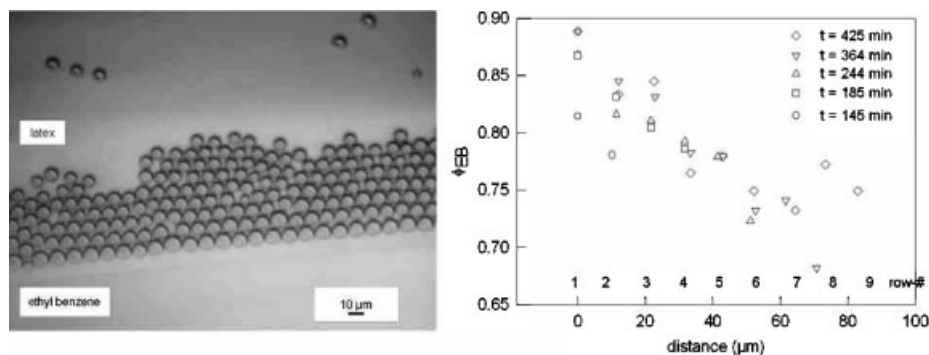


**Figure 7.**

Light microscopy image of polystyrene particles in contact with ethyl benzene (5 hours after contacting) and change of the volume fraction of ethyl benzene per particle in dependence on the distance from the interface between the latex and ethyl benzene at different times; the diameter of the unswollen particles is  $5.8 \pm 0.5 \mu\text{m}$ .

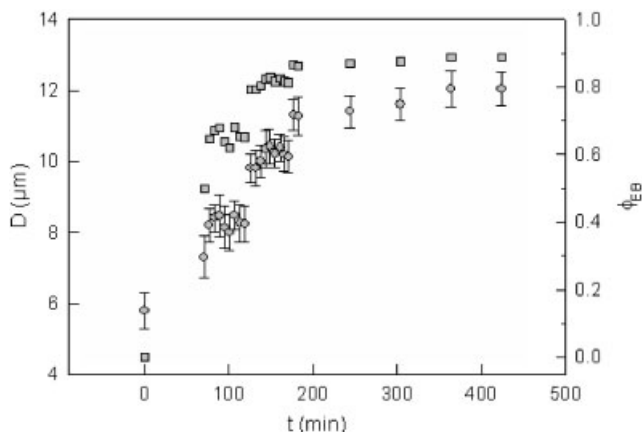


**Figure 8.**

Swelling kinetics of polystyrene particles with ethyl benzene at room temperature expressed as increase in the diameter ( $D$ , spheres) and volume fraction of ethyl benzene ( $\phi_{EB}$ , squares).

which is compensated by using an unrealistic high interfacial tension as discussed in.<sup>[14,19]</sup>

Two interesting experimental observations made during the light microscopy investigations are noteworthy. First, Latex particles sitting in the first row are captured from time to time by the organic phase. Thus, at equilibrium swollen latex particles are in contact with a polymer solution and not with a neat solvent phase. During swelling the chemical potential of the solvent in the particles increases and that of the solvent phase decreases until it is equi-

brated. Second, swelling of latex particles is cooperative in nature. This means that if a solution is in contact instead of a pure solvent also solute molecules are transferred into the latex particles. This happens even if the solute is a polymer as demonstrated by the images of Figure 9 proving the transfer of pyrene-labelled poly(methyl methacrylate) into polystyrene particles. These results have important consequences for carrying out emulsion polymerization and for the modification of polymer latexes. Obviously, there is a possibility to produce composite latex particles simply by swelling

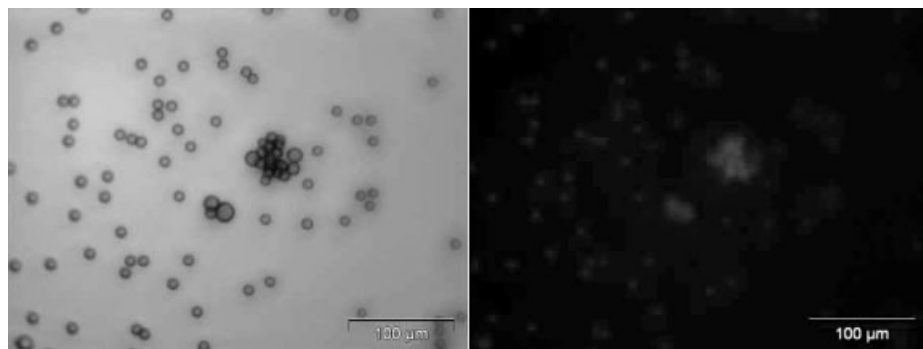


**Figure 9.**

Light microscopy images of swollen polystyrene latex particles; left: bright field image; right: fluorescence light image; the polystyrene particles are in quiescent contact with a solution of poly[(pyrenyl methacrylate)-co-(methyl methacrylate)] in ethyl benzene; images were taken about one week after contacting the latex with the copolymer solution; the pyrene-labelled copolymer was prepared as described in.<sup>[21]</sup>

with appropriate solutions. In monomer-flooded polymerizations the monomer phase will always contain a certain amount of polymer either as result of the capture of latex particle by monomer droplets or as result of direct polymerization inside the monomer droplets as also radicals can be captured.

For the uptake of radicals by latex particles four mechanisms are discussed differing regarding the dependence of the capture rate coefficient ( $k_c$ ) on the particle size ( $k_c \propto D^\alpha$ ). The collision model predicts  $\alpha = 2$ ,<sup>[22,23]</sup> the diffusion model  $\alpha = 1$ ,<sup>[24,25]</sup> the colloidal model also  $\alpha = 1$ ,<sup>[26]</sup> and the propagational model  $\alpha = 0$ .<sup>[27]</sup> Interestingly, experimental results have been published proving the validity of all models. Obviously, each of these models is only valid for a certain range of experimental conditions. This is an insufficient situation showing that the general behavior regarding the absorption of matter by latex particles has not yet been understood.

Recently, a way out of this state has been found by investigating the capture kinetics with Brownian dynamics simulations as described in.<sup>[28]</sup> These numerical experiments allow effective simulation of a variety of experimental conditions regarding the size and the concentration of the particles. Note, models relying on the Smoluchowski equation are insufficient as it is valid for a single particle at infinite dilution.<sup>[29]</sup> However, in real emulsion polymerizations the volume fraction of the polymer particles ( $\phi_p$ ) can be well above 50%. With the Brownian dynamics simulations the capture time ( $\tau$ ) of a species by particles was numerically determined. ( $\tau$ ) is the time between the introduction of the particular species in the system and its irreversible capture by the particles. The capture rate constant  $k_c$  relates with ( $\tau$ ) according to equation (1) where  $N$  is the particle number and  $N_A$  is Avogadro's number.

$$k_c = \frac{N_A}{N\langle\tau\rangle} \quad (1)$$

The numerical simulations revealed that  $k_c$  depends on the particles size with

a power which itself changes effectively with the polymer volume fraction. For very low polymer volume fraction  $k_c \propto D$  ( $\alpha = 1$ ) as predicted by the Smoluchowski equation (2) where  $\tilde{D}_r$  is the diffusion coefficient of the absorbed species with a size much smaller than the particles.

$$k_c = 2\pi\tilde{D}_rDN_A \quad (2)$$

However, with increasing polymer volume fraction  $k_c$  increases above the value given by equation (2). Thus, a dimensionless number,  $Sm$  (Smoluchowski number), can be defined (equation (3)) relating the actual  $k_c$  - value to  $2\pi\tilde{D}_rDN_A$ .

$$Sm = \frac{k_c}{2\pi\tilde{D}_rDN_A} \quad (3)$$

The numerical results of the calculations (cf. Figure 10) for a wide range of  $D$  and  $N$  values can be nicely fitted by equation (4) where  $v = 17.95$  for the particular (geometrical) conditions of the simulation.

$$Sm = 1 + v\phi_p \quad (4)$$

The polymer volume fraction can be modified by the two independent variables particle size and particle number. For extremely low volume fractions the radical capture is determined by the Smoluchowski equation.

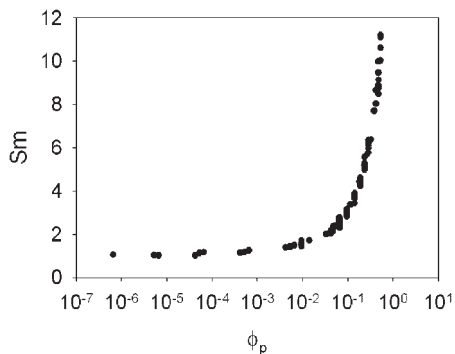


**Figure 10.**

Dependence of the capture rate of small molecules by particles in a polymer dispersion expressed by the Smoluchowski number ( $Sm$ ) on the polymer volume fraction ( $\phi_p = \frac{\pi/6 \cdot D^3 \cdot N}{\pi/6 \cdot D^3 \cdot N + v_w}$ ); the dispersion is composed of water with the volume  $v_w$  and polymer particles with the overall volume ( $N \cdot (\pi/6) \cdot D^3$ ).

Moreover, the absorption or capture rate depends on the size of the absorbed species as expressed by their diffusion coefficients ( $\bar{D}_r$ ). The smaller the species are the higher is the capture rate by the larger particles as verified by numerical simulations. Moreover, the simulations show that the capture rate depends on the relative position of the absorbed species to the particle. The closer to the particle surface the species is generated or born or introduced the higher the capture rate. This is clearly in accordance with experimental data as shown exemplarily in Figure 10.

## Conclusions

Conductivity measurement is an extremely useful tool to identify the mechanism of particle nucleation. The experimental data obtained so far give no hint that micelles of low molecular weight surfactants are a major locus of particle formation. The data show that particle nucleation takes place outside the micelles and can be understood as aggregative nucleation within the frame of the classical nucleation theory.<sup>[9]</sup> However, the presence of seed particles can effectively prevent the formation of new particles as, above a critical volume fraction, they act as absorbers for any kind of smaller-sized matter present in the dispersion. Brownian dynamics simulations suggest that any kind of species (radicals, monomers oligomers) can enter latex particles in dependence on their size for a given polymer volume fraction. In this sense and in contradiction to the propagational entry model<sup>[27]</sup> primary radicals can enter latex particles as it was proven also experimentally<sup>[30]</sup>. Swelling of latex particles with monomer must not necessarily take place via the uptake of single molecules as also monomer droplets are present in the aqueous phase. This spontaneous emulsification that takes place if two immiscible liquids are present<sup>[16]</sup> has enormous consequences for the mechanism of emulsion polymerization, not only for swelling but also for particle formation and morphology.

**Acknowledgements:** The authors gratefully acknowledge financial support from the Max Planck Society and technical assistance from Mrs. Ursula Lubahn, Mrs. Sylvia Pirok, Mrs. Rona Pitschke, Mrs. Heike Runge, and Mrs. Eugenia Maximova (MPI of Plant Physiology). O. L. is thankful for a fellowship provided by the German Academic Exchange Service (DAAD) within the Michail Lomonosov Program.

- [1] D. Urban, D. Distler, in: “*Polymer Dispersions and Their Industrial Applications*”, D., Urban, K. Takamura, Wiley-VCH Verlag GmbH, Weinheim **2002**, p. 1–14.
- [2] K. Tauer, M. Antonietti, L. Rosengarten, H. Müller, *Macromol. Chem. Phys.* **1998**, 199, 897–908.
- [3] R. Walz, B. Bömer, W. Heitz, *Makromol. Chem. Macromol. Chem. Phys.* **1977**, 178, 2527–2534.
- [4] I. Kühn, K. Tauer, *Macromolecules* **1995**, 28, 8122–8128.
- [5] S. Kozempel, thesis “Emulgatorfreie Emulsionspolymerisation – Monomerlösungszustand und Teilchenbildung”, Mathematisch-Naturwissenschaftlichen Fakultät, University of Potsdam, Potsdam, Germany, **2005**.
- [6] K. Tauer, R. Deckwer, I. Kühn, C. Schellenberg, *Coll. Polym. Sci.* **1999**, 277, 607–626.
- [7] K. Tauer, I. Kühn, *NATO ASI Series, Series E: Applied Sciences* **1997**, 335, 49–65.
- [8] K. Tauer, I. Kühn, H. Kaspar, *Progr. Coll. Polym. Sci.* **1996**, 101, 30–37.
- [9] K. Tauer, I. Kühn, *Macromolecules* **1995**, 28, 2236–2239.
- [10] R. M. Fitch, R. C. Watson, *J. Coll. Interf. Sci.* **1979**, 68, 14–20.
- [11] K. Tauer, M. Mukhamedjanova, C. Holtze, P. Nazaran, J. Lee, *Macromol. Symp.* **2007**, 248, 227–238.
- [12] W. D. Harkins, *J. Amer. Chem. Soc.* **1947**, 69, 1428–1444.
- [13] W. V. Smith, R. H. Ewart, *J. Chem. Phys.* **1948**, 16, 592–599.
- [14] K. Tauer, H. Kaspar, M. Antonietti, *Coll. Polym. Sci.* **2000**, 278, 814–820.
- [15] S. Kozempel, K. Tauer, G. Rother, *Polymer* **2005**, 46, 1169–1179.
- [16] K. Tauer, S. Kozempel, G. Rother, *J. Coll. Interf. Sci.* **2007**, 312, 432–438.
- [17] K. Tauer, S. Nozari, A. M. I. Ali, S. Kozempel, *Macromol. Rapid Commun.* **2005**, 26, 1228–1232.
- [18] M. Morton, S. Kaizerman, M. W. Altier, *J. Coll. Sci.* **1954**, 9, 300–312.
- [19] M. Antonietti, H. Kaspar, K. Tauer, *Langmuir* **1996**, 12, 6211–6217.
- [20] B. R. Vijayendran, *J. Appl. Polym. Sci.* **1979**, 23, 733–742.
- [21] N. Saito, Y. Kagari, M. Okubo, *Langmuir* **2006**, 22, 9397–9402.
- [22] R. M. Fitch, C. H. Tsai, *Polym. Coll. Proc. Symp.* **1971**, 73–102.

- [23] J. L. Gardon, *J. Polym. Sci., A-1 Polym. Chem.* **1968**, 6, 623–8.
- [24] F. K. Hansen, J. Ugelstad, *J. Polym. Sci., A-1 Polym. Chem.* **1978**, 16, 1953–1979.
- [25] J. Ugelstad, F. K. Hansen, *Rubb. Chem. Tewchnol.* **1976**, 49, 536–609.
- [26] I. A. Penboss, R. G. Gilbert, D. H. Napper, *J. Chem. Soc. Faraday Trans.* **1986**, 82, 2247–2268.
- [27] I. A. Maxwell, B. R. Morrison, D. H. Napper, R. G. Gilbert, *Macromolecules* **1991**, 24, 1629–1640.
- [28] H. F. Hernandez, K. Tauer, *Ind. Eng. Chem. Res.* **2007**, 46, 4480–4485.
- [29] M. von Smoluchowski, *Ann. Physik* **1906**, 21, 756–780.
- [30] K. Tauer, S. Nozari, A. M. I. Ali, *Macromolecules* **2005**, 38, 8611–8613.